NEW ADVANCES IN THE EXPERIMENTAL STUDIES OF THE ^{46}Mn β^+-DECAY CHANNEL AND ITS CONNECTION TO CCSNe IN LISE@GANIL*

D. Godos [a,b], L. Acosta [c], P. Ascher [d], B. Blank [d]
J. Giovinazzo [d], F. de Oliveira [e], C. Fougères [f,g]
A.M. Sánchez-Benítez [b]

[a]Instituto de Física, Universidad Nacional Autónoma de México
Circuito de la Investigación Científica
Ciudad Universitaria, 04510, Mexico City, Mexico
[b]Departamento de Ciencias Integradas
Centro de Estudios Avanzados en Física, Matemáticas y Computación
GIFMAN, UHU, Unidad Asociada al CSIC por el IEM
Universidad de Huelva, 21071, Huelva, Spain
[c]Instituto de Estructura de la Materia, CSIC, 28006, Madrid, Spain
[d]LP2i, 19 chemin du Solarium, 33170, Gradignan, France
[e]GANIL, Bd Henri Becquerel, 14000, Caen, France
[f]CEA, DAM, DIF, 91297 Arpajon, France
[g]Université Paris-Saclay, CEA
Laboratoire Matière en Conditions Extrêmes (LMCE)
Bruyères-le-Châtel, 91680, France

Received 31 October 2025, accepted 21 January 2026,
published online 31 March 2026

During the E666 experiment at the GANIL facility in 2016, where the fragmentation technique of a primary ^{58}Ni beam was used, ^{46}Mn, as well as other isotopes, was created and later implanted in a DSSSD surrounded by HPGe clovers. The subsequent β^+-decay could populate ^{46}Cr excited states above the proton separation energy, and later decay into ^{45}V in a process called β-delayed proton emission. The detection of the γ rays and protons emitted after the ^{46}Mn decay allowed us to study the inverse reaction to the ^{45}V$(p,\gamma)^{46}$Cr process. This later reaction impacts the ^{44}Ti production in Supernovae events. In this work, we present the preliminary results regarding the refined energy spectrum for the γ rays and charged particles detected, linked to the ^{46}Mn β^+-decay.

DOI:10.5506/APhysPolBSupp.19.1-A12

1. Introduction

The ^{44}Ti nucleosynthesis has certain characteristics that makes it a good γ-tracer for Supernovae events of the type of Core Collapse Supernova

* Presented at the XXXVIII Mazurian Lakes Conference on Physics, Piaski, Poland, August 31–September 6, 2025.

(CCSN) explosions[1]. First, the ^{44}Ti nucleosynthesis emits γ rays that are detected in γ-telescope satellites orbiting the Earth. Due to the ^{44}Ti relatively short half-life ($T_{1/2} \approx 60$ years), the γ-rays detection allows us to account for new CCSN events. This is important for the study of CCSN explosions, as the comparison between observations and models of the synthesized ^{44}Ti in CCSN explosions gives us constraints on the latter (the explosion energy and duration, the remnant, and ejected masses, *etc.*). Within the models of nucleosynthesis occurring in the last stages of CCSN progenitor stars, reaction networks are used employing thermonuclear reaction rates as their inputs [1–3], as well as masses and half-lives.

In this context, the ^{44}Ti nucleosynthesis in CCSN explosions is believed to be sensitive to the ^{45}V$(p,\gamma)^{46}$Cr reaction [4–6]. Nevertheless, reaction rates are very difficult to study in a direct way by the current nuclear laboratories. Therefore, indirect methods such as the quest for resonant contributions by means of the β-delayed proton emission technique may help [1, 7].

Hereby, we present the preliminary results of studying the resonant contributions to the ^{45}V$(p,\gamma)^{46}$Cr reaction rate by means of the ^{46}Mn β^+ decay channel. To do so, we have selected ^{46}Mn among other species in the cocktail beam delivered by the LISE fragment separator at GANIL (Caen, France), and later studied the excited states of its daughter nucleus ^{46}Cr. As part of our preliminary results, we present the proton and γ emission spectra related to the ^{46}Mn decay, comparing them with previous works from [8, 9].

2. Methodology

A ^{58}Ni^{26+} primary beam at 75 MeV/u was delivered with a 3 eμA current to the 230 mg/cm^2 $^{\text{nat}}$Ni production target during the "Isospin mixing in pf-shell proton emitters" (Code: E666; spokeperson: Bertram Blank, from LP2i Bordeaux) measurement of 2016 at LISE@GANIL. The resultant products of the fragmentation reaction continued their path through the fragment separator LISE (from the French, Ligne d'Ions Super Epluchées) selecting ^{45}Cr and its close isotopes for implantation in the detection setup. The detection setup consisted of a 297 μm silicon detector, a 316 μm double-sided silicon strip detector (DSSSD), and a 5 mm Si(Li) detector. The different fragments stopped in the middle of the DSSSD, but the SiLi acted as a *veto* for the fragments with enough energy to escape the DSSSD. The silicon detectors were surrounded by 4 HPGe clovers. The whole setup is sketched in Fig. 1.

[1] The CCSN explosions are the final process experienced by stars with an initial mass greater than 8 $M_\odot$.

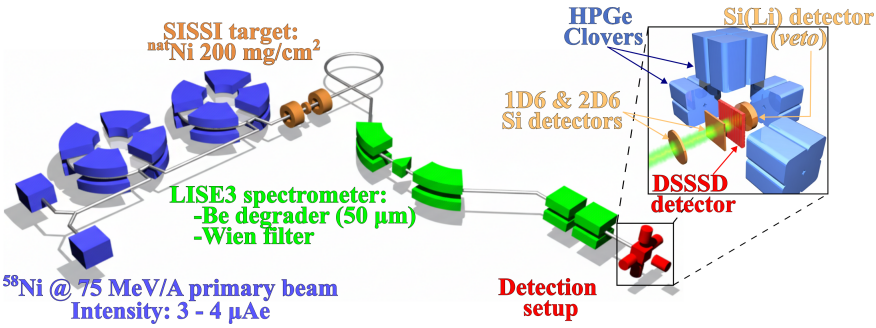

Fig. 1. Diagram of the LISE@GANIL beamline and depiction of the detection setup. Modified from [10].

2.1. Calibration of the detectors

The 32 DSSSD strips (16 from the P, and 16 from the N side) were calibrated using a triple α-source (^{239}Pm, ^{241}Am, and ^{244}Cm). Later on, this calibration was refined using proton emission peaks of well-known nuclei produced during the measurement (^{49}Fe, ^{45}Cr, ^{41}Ti, and ^{50}Co). The beta detection efficiency of the DSSSD strips was obtained using pure beta emitters that were also produced in the measurement (^{46}Cr and ^{42}Ti). In the case of the proton detection efficiency, it was considered to be 100% for protons with $E_p < 4$ MeV, while for higher energies, the efficiency drops.

In the case of the 4 HPGe clovers, we used ^{56}Co, ^{60}Co, ^{207}Bi, and ^{133}Ba+^{137}Cs sources to calibrate the 16 crystals. Their γ peaks were useful to obtain the γ efficiency at the respective energies, which were used to interpolate the γ efficiency values at any energy.

2.2. Isotope identification

As the experiment was run using a continuous beam, implantation and decay events happened at the same time. Therefore, both implantations and decays were triggering the acquisition. We could distinguish between them by means of the different triggers of the data acquisition, *i.e.*, a decay event would only trigger the acquisition by the DSSSD signal. On the contrary, an implantation event would trigger, in addition, other detectors upstream of the beamline. Furthermore, the last silicon detector, a Si(Li) detector, worked as a veto for fragments which, due to their high energy, were not implanted in the DSSSD.

In order to identify the implanted ions in the DSSSD, we used the ΔE — time of flight (ToF) technique. The energy loss in one of the silicon detectors was used together with the difference of the clock stamp of the cyclotron and the one of the particle passing by a reference detector. The 1D6 detector alongside CAVIAR, a multi-wires proportional detector composed

by 96 wires at a 15 mbar isobutene pressure that was placed upside the beamline, were used to establish two different graphical selection windows for each isotope. An example is shown in Fig. 2.

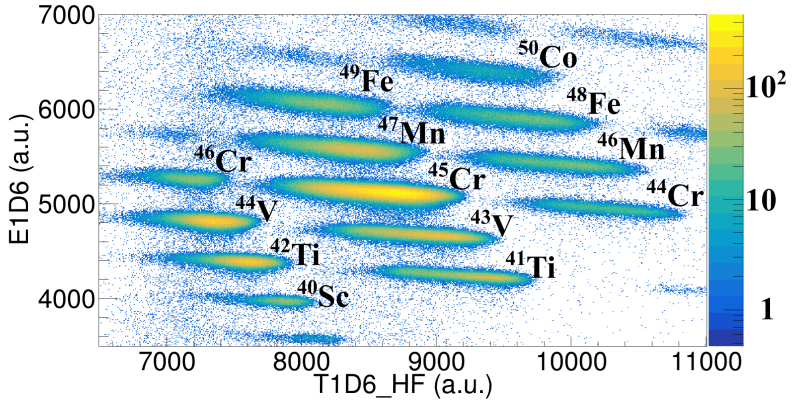

Fig. 2. ΔE — ToF technique with the Si detector labeled E1D6. Modified from [10].

After selecting one type of implanted isotope, such as ^{46}Mn, the energy spectra associated with its decay by spatial and time correlations were obtained. For time correlation, a time window T_w of several times the half-life was opened before and after one implantation event. The time windows used were $T_w = 1$ s for ^{46}Mn ($T_{1/2} = 36.2(4)$ ms), and $T_w = 6$ s in the case of ^{46}Cr ($T_{1/2} = 244.3(4)$ ms), and ^{42}Ti ($T_{1/2} = 208.3(6)$ ms) [11, 12]. Then, a correlation was made with all decay-type events that occurred during that time window. The negative time difference accounted for a signal background, as only random coincidences take place in this negative time window. For the spatial correlation, as the DSSSD vertical and horizontal strips form a grid of pixels, the implantation coordinates were used to select only the decay events that occur in the same pixel of the DSSSD as the isotope of interest. In addition, we only considered isotopes implanted in the central strips of the DSSSD [13].

Moreover, from the time difference histogram, we can measure the half-life of the isotopes. Exponential fits were used, considering the contribution of the daughter nuclei, to obtain the respective half-lives.

3. Preliminary results

3.1. Energy spectra of the DSSSD and HPGe detectors

The resultant energy spectra related to the ^{46}Mn β^+-decay, using the above method, can be seen in Figs. 3 and 4. Labeled with numbers, the

peaks previously seen by [8] are shown; meanwhile, the dotted lines show proton peaks seen by [14] with a time projection chamber (TPC); and the arrows mark new γ peaks not previously seen.

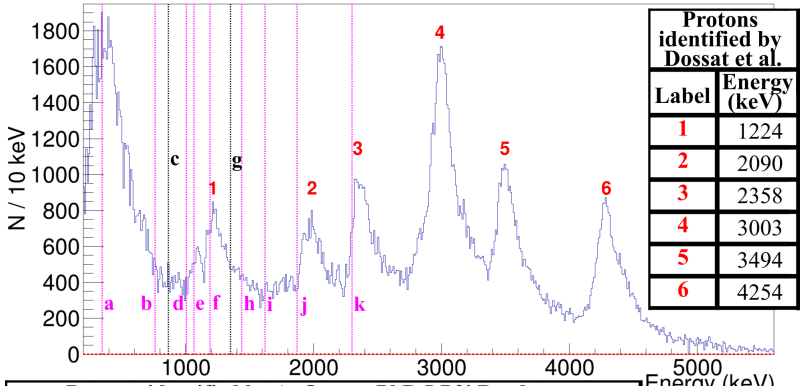

Protons identified by Dossat et al.	
Label	Energy (keV)
1	1224
2	2090
3	2358
4	3003
5	3494
6	4254

Protons identified by A. Ortega PhD LP2i Bordeaux											
Label	a	b	c	d	e	f	g	h	i	j	k
Energy (keV)	347	760	864	1005	1065	1191	1350	1440	1620	1870	2300

Fig. 3. Preliminary energy spectrum for the DSSSD strips from 40 keV to 5500 keV. The tables show the peak energies previously found in [8] and [14]. The c and g labels are identified as contamination of ^{44}Cr in [14]. Modified from [10].

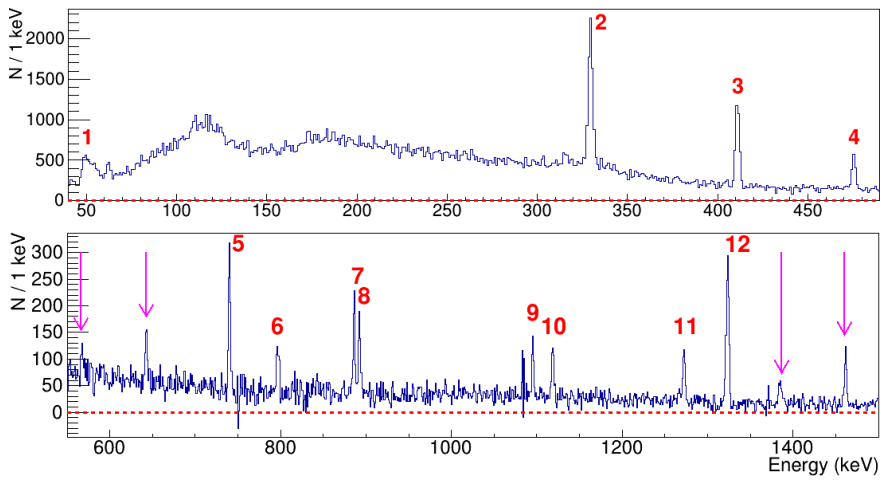

Fig. 4. (Color online) Preliminary energy spectrum for the HPGe crystals from 40 keV to 500 keV, and from 550 keV to 1500 keV. Gray/red numbers indicate peaks previously published in [8]. The arrows show new peaks found in this work. Modified from [10].

4. Conclusion

We have performed a study of the ^{46}Mn β^+-decay, obtaining the energy spectra for charged particles and γ rays. In these spectra, we see new details unseen in previous works [8, 9], like peak-alike structures in the γ rays spectrum. The above could mean that the ^{46}Mn decay scheme is very likely incomplete. Therefore, a deeper study on this decay is necessary. In addition, the potential proton peaks seen in [14] (ACTAR TPC) allow us to perform a p–γ analysis, which was not possible in [14] measurement due to the lack of γ detectors. As future work, we will focus on the γ rays and proton peaks coincidence analysis. This work is in progress.

This work was supported by the European Union's Horizon 2020 Framework research and innovation programme 654002 (ENSAR2) and by the Conseil Régional d'Aquitaine, France. This work was partially supported by DGAPA-UNAM IG101423, CONACyT 314857, MICIU PID2023-147569NB-C21, and MICIU PID2023-147569NB-C22 projects. We acknowledge the support from ASTRANUCAP, and the Centro de Estudios Avanzados en Física, Matemáticas y Computación of the University of Huelva, CEAFMC-UHU.

REFERENCES

[1] C. Illiadis, «Nuclear Physics of Stars», *Wiley-VCH*, Weinheim 2007.

[2] A. Heger *et al.*, *Astrophys. J.* **591**, 288 (2003).

[3] C. Giunti, K.C. Wook, «Fundamentals of Neutrino Physics and Astrophysics», *Oxford University Press*, New York 2007.

[4] L.S. The *et al.*, *Astrophys. J.* **504**, 500 (1998).

[5] K. Hermansen *et al.*, *Astrophys. J.* **901**, 77 (2020).

[6] G. Magkotsios *et al.*, *Astrophys. J.* **191**, 66 (2010).

[7] L. Trache *et al.*, *AIP Conf. Proc.* **1409**, 67 (2011).

[8] C. Dossat *et al.*, *Nucl. Phys. A* **792**, 18 (2007).

[9] J. Giovinazzo *et al.*, *Eur. Phys. J. A* **10**, 73 (2001).

[10] D. Godos-Valencia *et al.*, *EPJ Web Conf.* **275**, 02005 (2023).

[11] B. Singh, `https://www.nndc.bnl.gov/nudat3/getdataset.jsp?nucleus=46Cr&unc=NDS`

[12] B. Singh, J. Chen, `https://www.nndc.bnl.gov/nudat3/getdataset.jsp?nucleus=46Cr&unc=NDS`

[13] S.E.A. Orrigo *et al.*, *Phys. Rev. C* **93**, 044336 (2016).

[14] A. Ortega, «Two proton radioactivity and other exotic decays in the ^{48}Ni region measured with ACTAR TPC», Université de Bordeaux, Bordeaux, 2023.